

## Non-Contact Energy Harvesting for Rural Grade Crossings - Year 2

Joseph A. Turner, Ph.D.

Kirby Gray (Battelle) Chair in Engineering

Professor of Aerospace Engineering, Iowa State University

Emeritus Professor of Mechanical and Materials Engineering

University of Nebraska-Lincoln

Mohsen Amjadian, Ph.D.

Assistant Professor

Civil Engineering

University of Texas Rio Grande Valley

Carl Nelson, Ph.D.

Professor

Mechanical and Materials Engineering

University of Nebraska-Lincoln

Prince Mensah

Graduate Research Assistant

Mechanical and Materials Engineering

University of Nebraska-Lincoln

A Report on Research Sponsored by

University Transportation Center for Railway Safety (UTCRS)

University of Nebraska-Lincoln (UNL)

January 2026

## Technical Report Documentation Page

1. Report No. UTCRS-UNL-M5CY24	2. Government Accession No.	3. Recipient's Catalog No.	
4. Title and Subtitle Non-Contact Energy Harvesting for Rural Grade Crossings - Year 2		5. Report Date January 31, 2026	
		6. Performing Organization Code UTCRS-UNL	
7. Author(s) Joseph A. Turner, Mohsen Amjadian, Carl Nelson, and Prince Mensah		8. Performing Organization Report No. UTCRS-UNL-M5CY24	
9. Performing Organization Name and Address University Transportation Center for Railway Safety (UTCRS) Mechanical and Materials Engineering University of Nebraska-Lincoln (UNL) W342 Nebraska Hall Lincoln, NE 68588		10. Work Unit No. (TRAIS)	
		11. Contract or Grant No. 69A3552348340	
12. Sponsoring Agency Name and Address U.S. Department of Transportation (USDOT) University Transportation Centers Program 1200 New Jersey Ave. SE Washington, DC, 20590		13. Type of Report and Period Covered Project Report September 1, 2024 – December 31, 2025	
		14. Sponsoring Agency Code USDOT UTC Program	
15. Supplementary Notes			
16. Abstract The network of US railroads often spans remote parts of the country that are sparsely populated. In these areas, rail grade crossings are much less likely to have warning lights or crossing gates primarily due to the lack of electricity. Such unprotected or passive crossings have the majority of the grade crossing fatalities and accidents. To reduce rail accidents, enhanced warning systems are needed at as many passive crossings as possible. We propose to create a new energy harvesting approach based on the motion of the wheels to generate sufficient power for an LED-based grade crossing warning system. Recent advances to create small and powerful magnets allow for the design of a non-contact power generation approach that is activated with each passing wheel. The feasibility of this approach was shown in the first year of this project. The experiment was then expanded in the second year to include a moving plate and an optimized coil which improved the induced voltage of the system. Also, a rectifier was incorporated to convert the AC voltage to a DC voltage. An initial prototype has been designed and manufactured. An electrical board will be designed and incorporated into the prototype for field testing to be conducted on a short line railroad during the third year of this project.			
17. Key Words Electric power generation, at grade intersections, rural areas, electromagnetic devices		18. Distribution Statement This report is available for download from <a href="https://www.utrgv.edu/railwaysafety/research/mechanical/index.htm">https://www.utrgv.edu/railwaysafety/research/mechanical/index.htm</a>	
19. Security Classification (of this report) None	20. Security Classification (of this page) None	21. No. of Pages 14	22. Price

## Table of Contents

<b>List of Figures</b> .....	3
<b>List of Tables</b> .....	3
<b>List of Abbreviations</b> .....	4
<b>Disclaimer</b> .....	4
<b>Acknowledgements</b> .....	4
<b>1. Introduction</b> .....	5
<b>2. Summary</b> .....	5
<b>3. Computational Model</b> .....	6
<b>4. Experiments</b> .....	9
<b>5. Prototype Design</b> .....	12
<b>6. Conclusions and Future Work</b> .....	13
<b>7. References</b> .....	14

## List of Figures

Figure 1: Finite Element Model (FEM) of the magnet and plate in COMSOL Multiphysics. ....	6
Figure 2: Two-dimensional COMSOL model of a moving magnet in a coil vicinity. ....	7
Figure 3: Computational model results for a speed of 45 mph. ....	8
Figure 4: Experimental setup to explore feasibility. ....	10
Figure 5: Experimental results .....	11
Figure 6: (A) Rectifier and (B) output from rectifier for continuous excitation.....	11
Figure 7: Prototype Design.....	12

## List of Tables

Table 1. Simulation results for different train speeds .....	8
--	---

## **List of Abbreviations**

DAQ	Data Acquisition
FE	Finite Element
FEM	Finite Element Model
FFT	Fast Fourier Transform
UTCRS	University Transportation Center for Railway Safety

## **Disclaimer**

The contents of this report reflect the views of the authors, who are responsible for the facts and the accuracy of the information presented herein. This document is disseminated under the sponsorship of the U.S. Department of Transportation's University Transportation Centers Program, in the interest of information exchange. The U.S. Government assumes no liability for the contents or use thereof.

## **Acknowledgements**

The authors wish to acknowledge the University Transportation Center for Railway Safety (UTCRS) for funding this project under the USDOT UTC Program Grant No. 69A3552348340.

## **1. Introduction**

A major goal of the UTCRS is devoted to a reduction in fatalities and overall accidents associated with rail transport. Rural rail crossings are often uncontrolled or “passive” which means that no signal lights or barriers are activated by an on-coming train. These types of crossings represent a large percentage of the total accidents that occur at roadway-rail intersections. The purpose of this project is to create an energy harvesting system that is located near the rail and is driven by the interaction with passing railcar wheels. According to the Institute of Transportation Engineers (2024), crossings with lighted signals require ~40 W of power so the goal for this project is very clear. The large number of passive crossings is primarily due to a lack of power in such remote locations. The proposed research is focused on a new approach to power generation that would provide sufficient energy for one or more signaling modalities in order to have cost-effective solutions for such an important safety need. A computational model was created, and a laboratory experiment was designed in the first year of this project to show that significant power could be generated with this approach. During the second year of this project, the laboratory experiment was modified for the power harvesting system to be excited by a moving steel plate with the help of linear guide rail. Here, the moving plate simulates the passing of a train wheel. An initial prototype was designed and manufactured. Optimization of the coil was done to improve the voltage induced in the coil. A rectifier was built and installed in the setup to convert the AC voltage from the coil to DC voltage. An initial prototype has been designed and the mechanical part manufactured. Now this prototype must be optimized and an electrical board made up of a rectifier, booster and a supercapacitor (to store the voltage/power) included in order to conduct field experiments.

## **2. Summary**

There is a high need for signal lights at passive rail crossings throughout the United States. Many prior designs required complex changes to the rail bed or were based on contact with components of the train. Our goal is to create a non-contact energy harvesting system that can be easily integrated with most rail crossings. In the first year of the project, the feasibility of this approach was studied computationally and experimentally with a positive outcome. The coil in the experimental setup was optimized to improve the induced voltage in the coil during the second

year. Also, a rectifier was introduced to convert the AC voltage to a DC voltage. Finally, an initial prototype has been designed and manufactured. An electrical board will be built to receive the output voltage from the rectifier and boost it to be stored by a supercapacitor during field testing.

### 3. Computational Model

In the second year of this project, a finite element (FE) model similar to that described in the previous report was developed to quantify the power based on parameters from the experimental setup which is discussed in the subsequent section of this report. The goal was to estimate the force amplitudes for different train speeds and their corresponding power that can be generated from them. First, a parametric study was conducted to estimate the profile and maximum force amplitude for the given mass and steel plate. The magnet was a neodymium counterbored ring magnet with a remanent flux density of 1.48 T and a relative recoil permeability of 1.05 (K&J Magnetics, 2024) and the steel plate with dimensions  $2 \times 2 \times 0.5$  in. The magnet has an outer diameter, major inner diameter and thickness of 1 in, 0.19 in and 0.5 in respectively, with a mass of 46.3 g and a height of 0.5 in. The mesh of the computational model and its corresponding force profile for a 0.5-inch interval are depicted in Figure 1A and B. The amplitude of the profile was verified with an analytical model developed by González (2016).

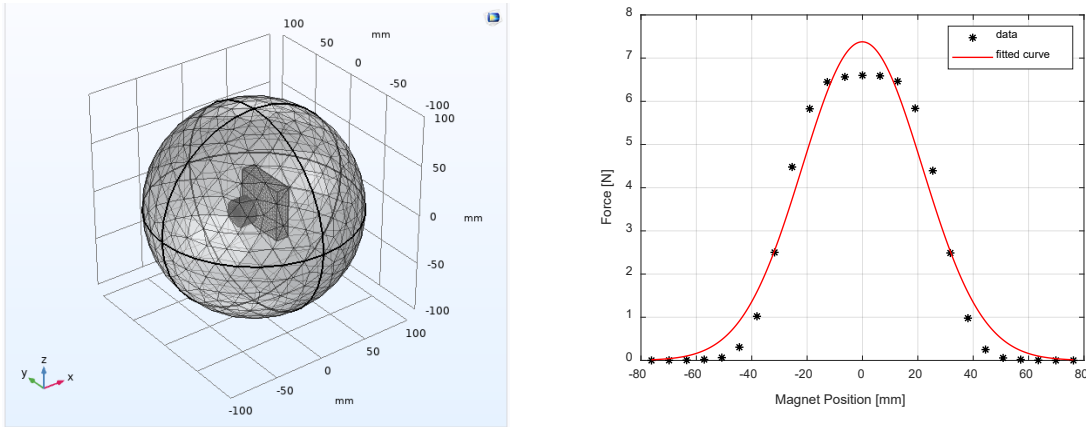


Figure 1: Finite Element Model (FEM) of the magnet and plate in COMSOL Multiphysics. The figure shown in (A) is the mesh of the model in COMSOL and the corresponding force profile for a parametric sweep of the plate across the magnet with 0.5-inch interval is shown in (B).

The COMSOL result suggested that typical train speeds would result in force inputs on the magnet that were close to impulsive. The impulse amplitude was defined in terms of the magnet-plate gap, and the power generation was defined relative to the optimized coil parameters (Amjadian et al. 2022, Halin et al. 2016, Bijak et al. 2022). The coil was made of a 33-gauge wire, had 700 turns and a height of 0.5 in. These parameters were then used to estimate the displacement of the magnet for different train speeds with the spring stiffness and damping coefficient determined from the experimental setup. Then, the power generated for each speed was quantified. The two-dimensional model utilized to estimate this power is depicted in Figure 2. The moving mesh feature in COMSOL was utilized to define the equivalent displacement for each case.

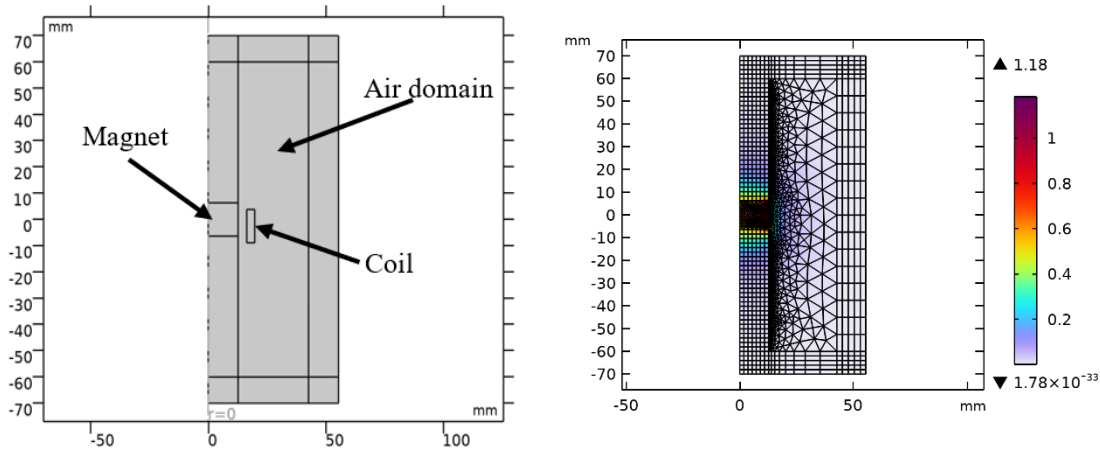


Figure 2: Two-dimensional COMSOL model of a moving magnet in a coil vicinity. The figure in (A) shows the geometry of the two-dimensional model. The figure in (B) shows the surface magnetic flux density of the model.

Figure 3A and B depict the induced voltage and instantaneous power for the case with a train speed of 45 mph (20.12 m/s). A single bogie excitation (two wheels) was considered in this simulation with excitation times for the first and second wheels being 0.10 and 0.22 s respectively. The maximum induced voltage for the first- and second-wheel excitations were 3.87 V and 3.99 V respectively. The corresponding maximum instantaneous powers were 289 and 308 mW respectively for the first- and second-wheel excitations. The average power for this speed was 77.36 mW for a single wheel excitation for a simulation time of 1 s.

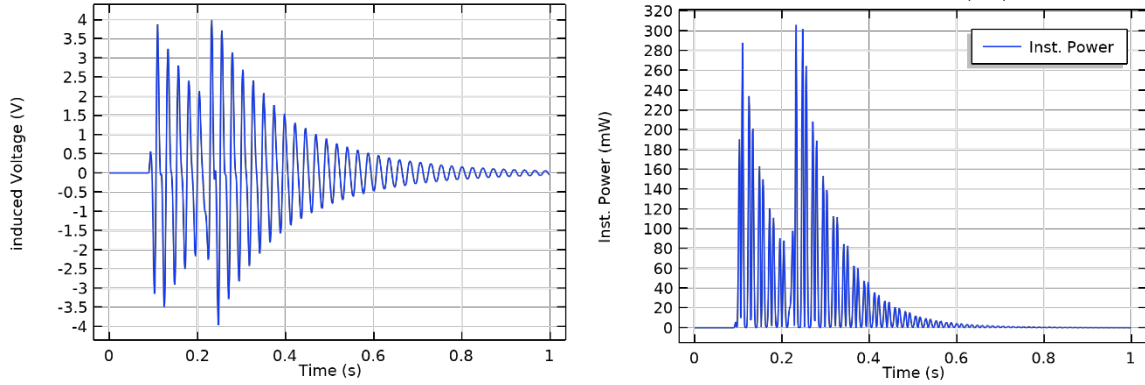


Figure 3: Computational model results for a speed of 45 mph. Figure (A) is the induced voltage from the simulation and that of (B) is the corresponding instantaneous power.

Table 1 summarizes the results from the simulation for different train speeds with a simulation time of one second.

Table 1: Simulation results for different train speeds

Speed [mph (m/s)]	Max. Disp. [mm]	Max. Voltage [V]	Max. Inst. Power [mW]	Avg. Power [mW]
25 (11.18)	4.84	8.73	1460.00	350.90
30 (13.41)	4.03	6.85	901.50	223.30
35 (15.65)	3.46	5.33	545.50	142.31
40 (17.88)	3.02	4.49	386.50	102.83
45 (20.12)	2.69	3.87	284.50	77.36
50 (22.35)	2.42	3.39	220.85	60.358
55 (24.59)	2.20	2.95	167.25	47.67
60 (26.82)	2.02	2.70	139.60	39.48
65 (29.06)	1.86	2.40	110.75	32.62
70 (31.29)	1.73	2.24	96.50	28.12
75 (33.52)	1.61	2.03	78.75	23.63
80 (35.76)	1.51	1.88	68.02	20.46

The results show that the induced voltage and average power decrease as speed increases for this sensor design. For speeds between 45 and 60 mph, the displacement amplitudes fall between 2 and 2.7 mm. These amplitudes correspond to maximum induced voltages of 2.7 to 3.9 V and maximum instantaneous power of 139.60 to 284.50 mW. These results were as expected based on the outcome of the experimental results.

#### 4. Experiments

A linear guide rail (as shown in Figure 4) was installed above the initial experimental setup with a steel plate ( $2 \times 2 \times 0.5$  in) mounted on it. The interval between the surface of the magnet and that of the steel plate was 0.5 in. The rail was used to simulate the passing of a train wheel by sliding the plate across the length of the rail. In this case, the mode of excitation of the system is the interaction force between the magnet and the moving plate. The magnet was a neodymium counterbored ring magnet with properties same as that discussed earlier in this report. The magnet was placed inside a coil. A gauge 33 wire was used to wind a coil of 700 turns on a coil fixture made of polymer. The complete setup is shown in Figure 5. Although the fundamental bending stiffness is controlled by the length, width, and thickness of the beam, the effective beam stiffness was increased by subjecting it to tension. Before the experiment was conducted, the mass was first displaced by hand and allowed to oscillate while the data were being recorded. The recorded data were then used to determine the frequency of the system by using fast Fourier transform (FFT). The damped frequency was also calculated using the response of the experiment together with the known parameters of the setup. The maximum permissible displacement of the magnet was obtained by recording its maximum displacement when the plate was positioned above the magnet. Once all the parameters had been found, the plate was then set in motion by pushing it along the rail to excite the magnet, and the induced voltage was recorded in LabVIEW through the data acquisition system.

Figure 5A illustrates the induced voltage from the experiment. The result shows that magnet oscillates and decays in about 1 second with an excitation frequency of 36.29 Hz and a maximum voltage of approximately 3.3 V. The corresponding instantaneous power from the induced voltage is depicted in Figure 5B. The maximum instantaneous power and average power were 287.8 and 47 mW respectively.

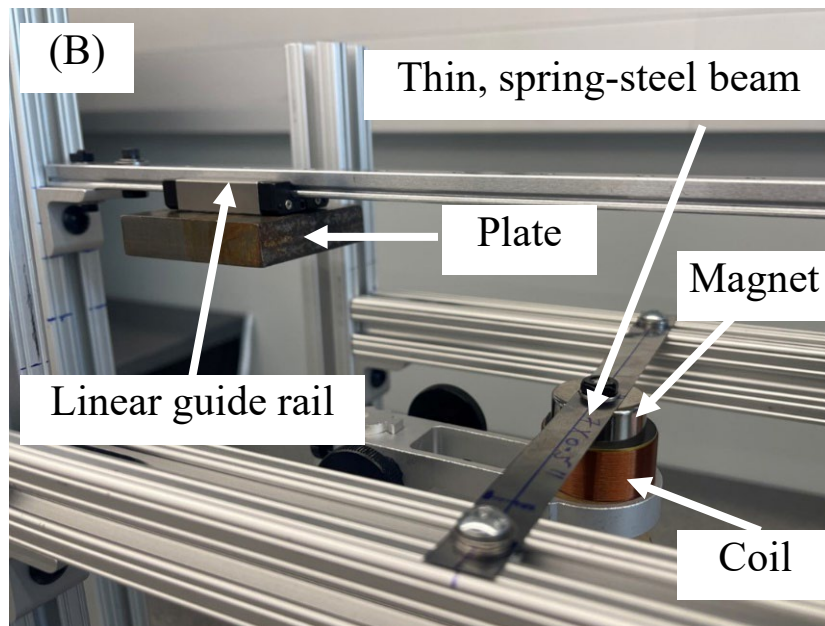
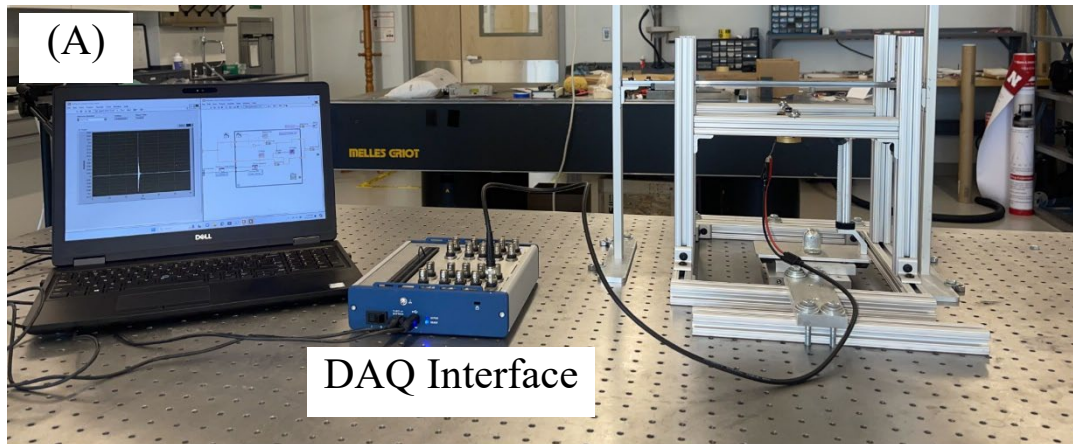


Figure 4: Experimental setup to explore feasibility. The view in (A) shows the whole setup. The data acquisition (DAQ) interface is connected to the coil to measure voltage as a function of time. The side view in (B) shows the magnet which oscillates within the coil to generate power together with the rail system and the mounted plate.

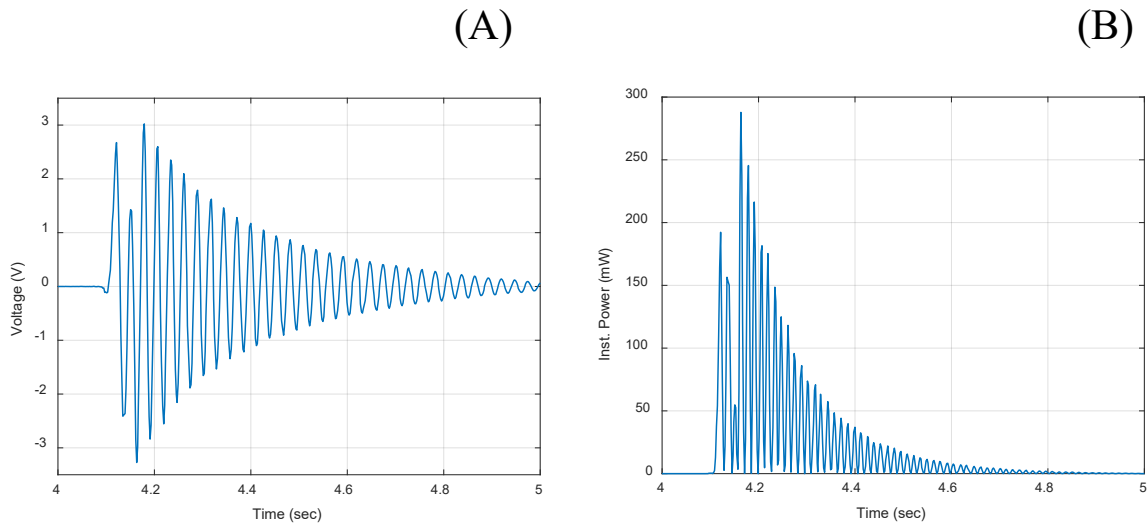


Figure 5: Experimental results

The result in (A) is the induced voltage in the coil from the experiment. The result shown in (B) is the corresponding instantaneous power from the results in (A).

A full-wave bridge rectifier, made of 4 1N5817 Schottky Diodes and a 1000  $\mu\text{F}$  capacitor, was designed and incorporated into the experimental setup. This rectifier was used to convert the AC voltage induced in the coil to a DC voltage. A continuous excitation was conducted by moving the plate back and forth for about 200 seconds and the output from the rectifier recorded. The rectifier circuit and the output for the continuous excitation from the rectifier are depicted in Figure 6A and B respectively.

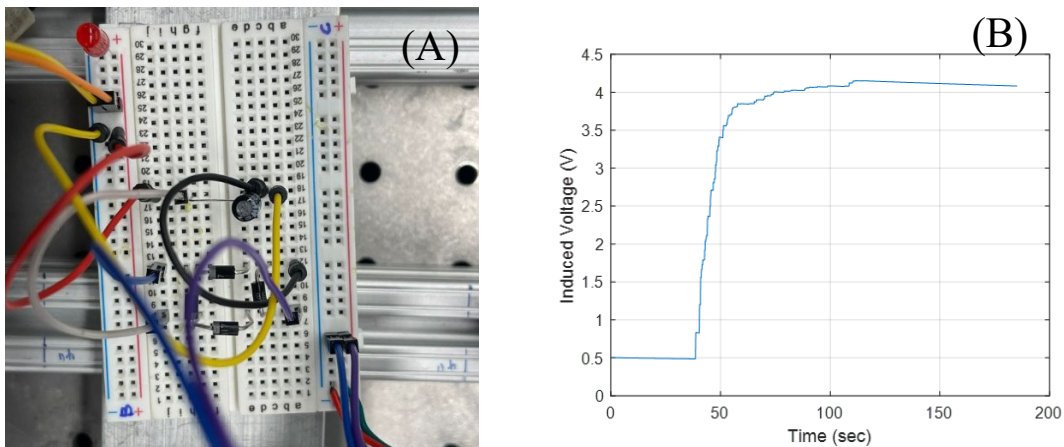


Figure 6: (A) Rectifier and (B) output from rectifier for continuous excitation

## 5. Prototype Design

A prototype has been designed and major parts manufactured. The main fixture that houses the magnet, coil and the spring steel was made of wood which is 0.75 inch thick. The base plate and the enclosure or casing were made of aluminum and acrylic respectively with both having a thickness of 0.25 in. Before settling on the casing material, experiments were conducted with aluminum and fiber glass placed between the magnet and the moving plate. The results show that these materials damp the response faster which made them unsuitable for the prototype casing. The CAD design, proposed installation and the manufactured prototype are depicted in Figure 7. An electrical board will be designed and incorporated into the prototype to finalize it for field testing. This board will include a rectifier to convert the AC voltage from the coil to a DC voltage, and a booster to increase the output voltage from the rectifier to a voltage that can charge a supercapacitor that will be included in the design. A supercapacitor will be utilized to store the voltage from the booster during the field testing.

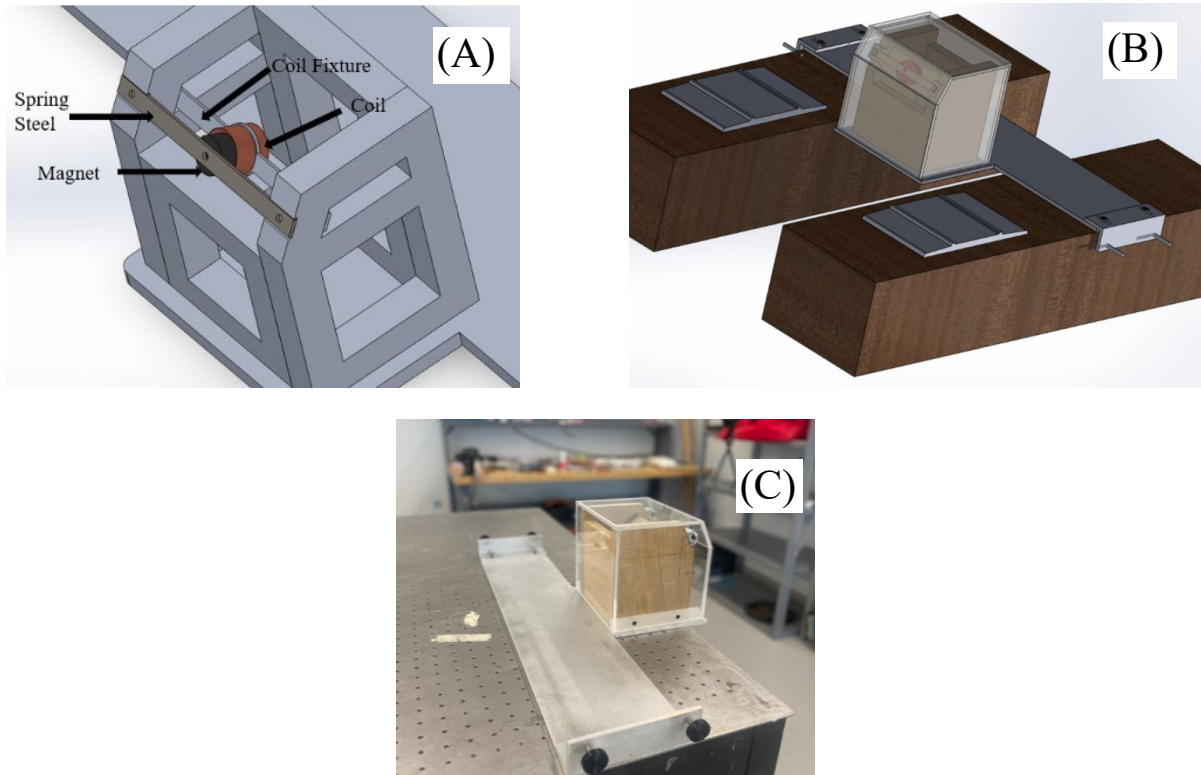


Figure 7: Prototype Design.

The view in (A) shows a CAD of the proposed prototype. The view in (B) shows the complete prototype and its proposed installation on the field. The view in (C) is the manufactured prototype.

## **6. Conclusions and Future Work**

The non-contact approach has continued to prove great value for field implementation but there is much more research yet to be accomplished. The preliminary experiment has been expanded to include a moving plate to simulate the passing of a train wheel. A coil fixture was designed to optimize the number of turns of the coil to produce a maximum induced voltage of approximately 3.3 V. With the inclusion of a rectifier and continuous excitation with the plate, the AC voltage was converted to a DC voltage with amplitude above 4 V. The specific experiment was modeled with COMSOL and the various speeds considered. The results show similarity between experimental and computational study for cases where the displacement amplitudes are almost the same for both the experimental and the computational studies. In the third year of this project, an electrical board made up of a rectifier and a booster will be designed, manufactured and incorporated into the prototype. Once this is achieved, initial field testing will be conducted. A supercapacitor will be installed in the output of the electrical board to store the power that will be generated from the field test. Also, a compliant mechanism will be designed and incorporated into the prototype to achieve a nominal optimized natural frequency. It will also simplify the relative motion of the magnet and coil by functioning as an integrated linear guide. Finally, our main objective for Year 3 is to finalize the prototype, conduct field experiments and analyze the data from the field test. A patent disclosure has been submitted.

## 7. References

Institute of Transportation Engineers, no date. *Grade crossing safety: Section 4B*. [online] Available at: <https://toolkits.ite.org/gradecrossing/sec04b.htm> [Accessed 29 Sep. 2024].

K&J Magnetics, Inc., no date. *Rod magnets*. [online] Available at: <https://www.kjmagnetics.com/rx038dcb-n52-neodymium-counterbored-ring-magnetc> [Accessed: 16 May 2024].

González, M. I., 2016. Forces between permanent magnets: experiments and model. *European Journal of Physics*, 38(2), p.025202.

Amjadian, M., Agrawal, A. K., & Nassif, H. H., 2022. Development of an analytical method for design of electromagnetic energy harvesters with planar magnetic arrays. *Energies*, 15(10), p.3540.

Halim, M. A., Cho, H., Salauddin, M., & Park, J. Y., 2016. A miniaturized electromagnetic vibration energy harvester using flux-guided magnet stacks for human-body-induced motion. *Sensors and Actuators A: Physical*, 249, p.23-31.

Bijak, J., Trawiński, T., & Szczygieł, M., 2022. Simulation and investigation of the change of geometric parameters on voltage induced in the energy harvesting system with magnetic spring. *Electronics*, 11(10), p.1639.